

Interannual variations of oceanographic and meteorological characteristics in the Sea of Okhotsk

Vladimir PONOMAREV¹, Olga Trusenkova¹, Elena Ustinova², and Dmitry Kaplunenko¹

¹ Pacific Oceanological Institute, Russian Academy of Sciences, Vladivostok, Russia

² Pacific Research Institute of Fisheries and Oceanography, Vladivostok, Russia

This study is devoted to low-frequency variations of oceanographic and meteorological characteristics in the Sea of Okhotsk. Time series of sea ice extent, air temperature at the meteorological stations around the Sea, South Oscillation Index (SOI), North Pacific Index (NPI), and of frequency of occurrence for certain meteorological situations were subjected to correlation and spectral analyses. Monthly and seasonal (winter and summer) mean time series were considered for the periods of 40 years and more. Both 3-month (December–February and June–August) and 5-month (November–March and May–September) averaging was used to compose the seasonal time series. In a few cases, averaging was performed for April–June, July–September, October–December or January–March. A 95%-confidence level was chosen to test statistical significance of estimates obtained.

Characteristic time-scales of low-frequency air temperature variations were obtained from power spectra for winter mean time series for the 20th century, often for more than 100 years. We chose the 3 following intervals of interest in the time-scale: biennial (2–3 years), ENSO (3–7 years), and decadal (7–13 years) intervals. Every chosen time interval has, as a rule, the only maximum of 95%-significance level in spectra for monthly mean time series. Typical examples are shown in Table 1. There are biennial maximums for the most stations in the most months. ENSO-scale maximums occur usually in spring, rarer in summer or fall and almost never in winter. On the contrary, decadal-scale maximums are often present in winter, and, rarer, in fall.

The situation is different from that in the Sea of Japan where ENSO-scale maximums are present in air temperature spectra for all seasons of a year, although both ENSO and decadal peaks usually do not occur simultaneously for the spectrum of the same month or season (Ponomarev et al., 1999). The spectrum for the Nemuro station (Table 1)

which is actually located at the Hokkaido Pacific coast is close to those for the Japan Sea. The presence of well-pronounced ENSO and decadal scale variations in the subarctic area corresponds to findings based on analysis of North Pacific winter sea surface temperature (Nakamura 1997; Ponomarev et al., 1999) as well as of the Oyashio Intrusion and snow coverage over eastern Asia (Sekine, Yamada, 1996). Thus, the relationship between seasonal air temperature anomalies and ENSO should be analyzed.

Unlagged cross-correlation was estimated between winter mean time series of air temperature at the meteorological stations around the Sea of Okhotsk and SOI. Lagged cross-correlation was estimated between winter mean air temperature and SOI for the previous (lag of –6 months) or next (lag of +6 months) summer. A statistically significant positive unlagged cross-correlation was found for stations located at the Sakhalin, Siberian and Kamchatka coasts of the Okhotsk Sea. A statistically significant positive lagged cross-correlation, air temperature lagging behind SOI (SOI taken for a previous summer), was also found, although smaller in value compared to the unlagged correlation. Examples are shown in Table 2. A chart of winter air temperature at the Ust-Hairuzovo meteorological station located at the Kamchatka coast of the Okhotsk Sea superimposed with SOI and NPI is shown in Figure 1. It also has unlagged and lagged (SOI leading 6 months) cross-correlations with SOI (Table 3).

Air temperature at the northern Okhotsk Sea shelf has an unlagged cross-correlation with SOI in a transitional fall–winter period from October to December (Table 4). Moreover, it also has a lagged correlation with SOI averaged both for July–September and April–June.

Thus, air temperature over the Sea of Okhotsk tends to have negative (positive) anomaly during winter El Niño (La Niña) events. Likewise, air

temperature over the Sea tends to have positive anomaly in winters following summer La Niña events. This conclusion, however, is not valid for some southern coastal Okhotsk Sea stations. As seen in Table 2, the Nemuro and Abashiri stations situated at the northeast Hokkaido coast do not have a statistically significant correlation with SOI, or with the most northern coastal stations in the Okhotsk Sea (Okhotsk and Magadan).

Low-frequency thermal regime variations also manifest themselves in the Okhotsk Sea ice. Sea ice winter mean time series (1957–1989) were composed by averaging 10-day ice cover in winter and early spring (21–28 of February, 1–10, 11–20

and 21–30 of March, and 1–10 of April). Both its unlagged and lagged (ice 6 months lagging SOI) cross-correlation with SOI is statistically significant and negative (Table 3, Fig. 2). Thus, ice cover in the Okhotsk Sea tends to increase during winter El Niño events (when SOI reaches its highest negative values) and to decrease in winters following summer La Niña events (when SOI reaches its highest positive values).

As a whole, seasonal links between ENSO and oceanographic and meteorological characteristics suggest winter cooling in the Sea of Okhotsk during winter El Niño events and winter warming there after previous summer La Niña events.

Table 1 Characteristic time-scales of air temperature variations for the meteorological stations around the Sea of Okhotsk based on seasonal mean time series spectra. A 95% confidence level is accepted. Underlined are values corresponding to the middle of ENSO (3.0–6.9) or decadal (7.0–13.5) periods.

Month	Station	Periods (in years)			Station	Periods (in years)			
		2.0–2.9	3.0–6.9	7.0–13.5		2.0–2.9	3.0–6.9	7.0–13.5	
Winter	Okhotsk, 1926–1990	2.2	6.4	8.0	Icha, 1951–1990	<u>2.0</u>	<u>4.0</u>	<u>9.3</u>	
Spring		2.1	<u>4.9</u>			2.9			
Summer						<u>2.0</u>			
Fall		2.0	3.0						
Winter	Ajan, 1951–1990	2.9	3.7 <u>5.6</u>	8.0	Simushir, 1951–1990	<u>2.0</u>	<u>5.0</u>	8.0	
Spring									2.0
Summer									<u>2.0</u>
Fall		2.4							2.4
Winter	Vakkanai, 1951–1990	2.9 2.4	<u>4.4</u>	8.0	Nemuro, 1884–1990	2.1	<u>4.1</u>	8.2 11.8	
Spring						2.5			
Summer						2.2			<u>5.6</u>
Fall						2.4			4.6
Winter	Yuzho- Sakhalinsk, 1951–1990	2.0	<u>5.0</u>	8.0	Abashiri 1951–1990	2.4	<u>5.0</u>	8.0	
Spring		2.0				3.1			
Summer									
Fall		2.4				13.3			2.4

Table 2 Cross-correlation of winter mean air temperature time series (1949–1990) at the coastal meteorological stations around the Sea of Okhotsk with each other and SOI averaged for the same winter, next summer (SOI, +6 months) and previous summer (SOI, –6 months). Linear trend is subtracted. A 95% confidence level is equal to 0.308, according to the Fisher test.

	Okhotsk	Ajan	Icha	Nikolaevsk	Alexndrvsk	Poronaysk	Abashiry	Nemuro	SOI	SOI, +6 mo	SOI, –6 mo
Magadan	0.93	0.53	0.79	0.42	0.43	0.52	none	none	0.54	none	0.43
Okhotsk		0.66	0.71	0.58	0.52	0.59	none	none	0.58	none	0.38
Ajan			0.48	0.68	0.78	0.69	0.4	0.47	0.41	none	none
Icha				0.46	0.57	0.59	0.46	0.47	0.51	none	0.42
Nikolaevsk					0.73	0.66	0.50	0.52	0.38	none	0.32
Alexndrvsk						0.84	0.71	0.75	0.42	none	0.28
Poronaysk							0.49	0.57	0.56	none	0.43
Abashiry								0.97	none	none	none
Nemuro									none	none	none

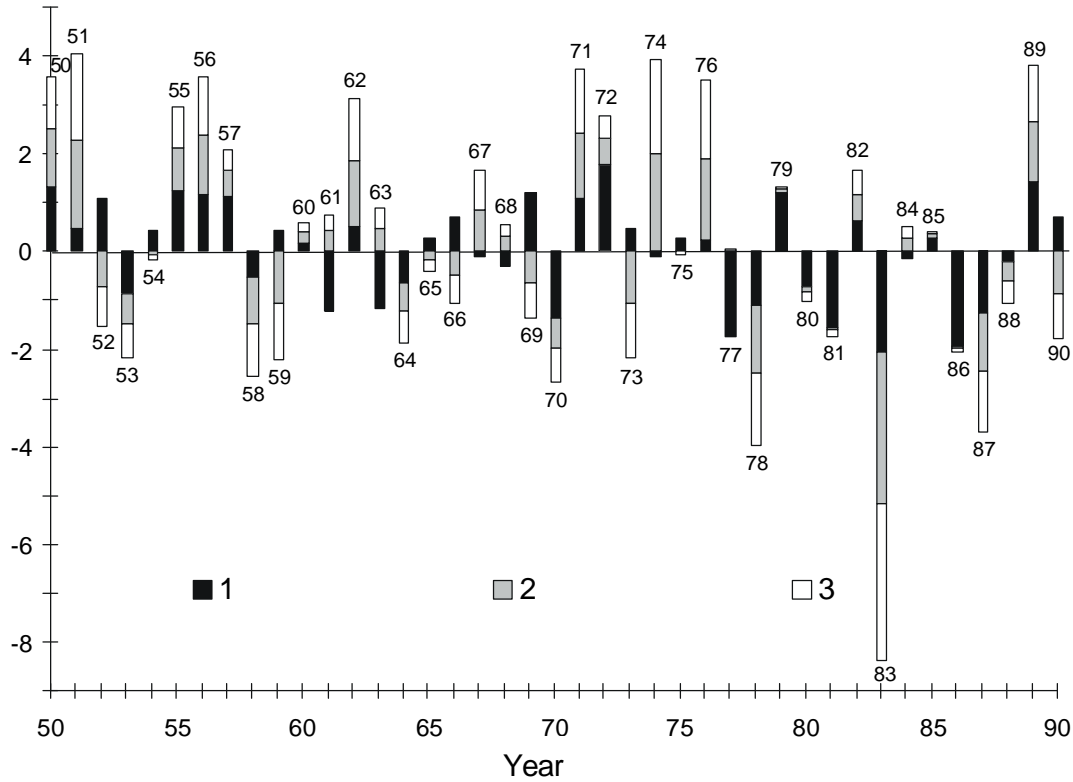


Fig. 1 Time series (1950–1990) of normalized winter anomalies of NPI (1), SOI (2), and air temperature at the Ust-Hairuzovo meteorological station (3). Positive anomalies of SOI correspond to La Niña events, negative anomalies correspond to El Niño events.

Table 3 Unlagged and lagged cross-correlation with SOI of some oceanographic and meteorological characteristics in the Sea of Okhotsk calculated for the winter mean time series. The 95% confidence levels are also shown, calculated based on the Fisher test.

Data	Unlagged SOI	SOI 6 months leading	95%-level
Ust-Hairuzovo air temperature, 1950–1990	0.55	0.34	0.312
Okhotsk sea ice, 1957–1990	-0.45	-0.46	0.349
North Pacific Index, 1940–1990	0.58	0.49	0.282

Table 4 Unlagged and lagged cross-correlation between air temperature at the coastal stations around the northern Okhotsk shelf averaged for October–December and SOI averaged for April–June (SOI, AMJ), July–September (SOI, JAS), October–December (SOI, OND) for the period from 1949 to 1990. A 95%-confidence level is equal to 0.308, according to the Fisher test.

	Ajan	Okhotsk	Magadan	Icha
SOI, AMJ	none	none	0.38	0.34
SOI, JAS	0.32	0.40	0.51	0.36
SOI, OND	none	0.47	0.56	none

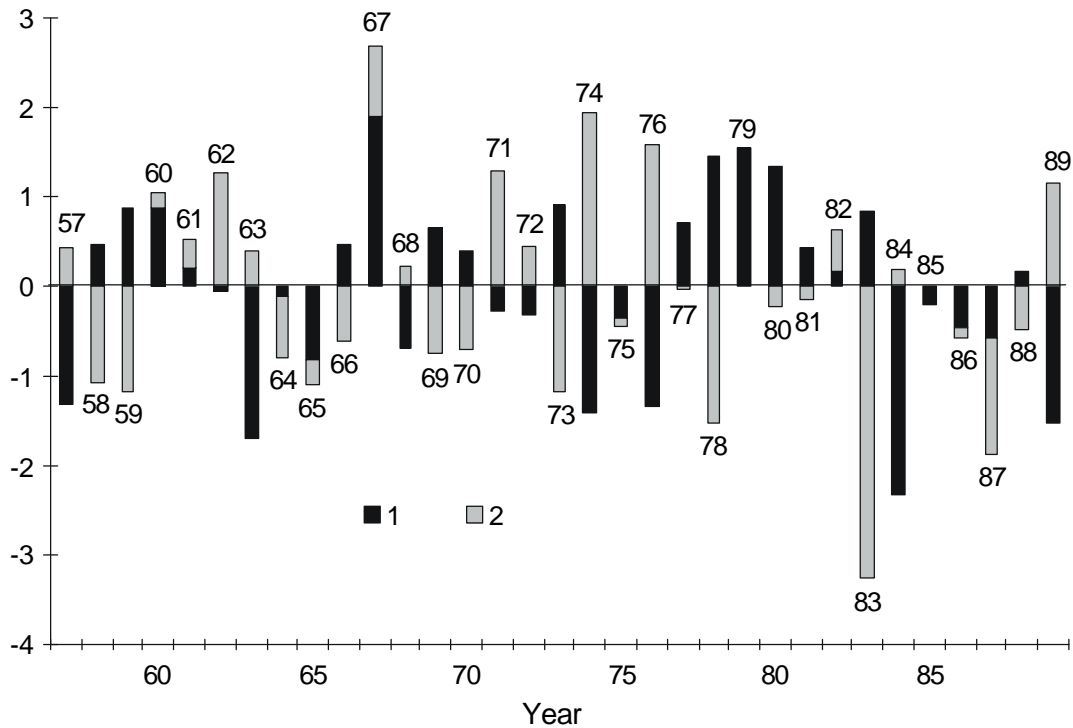


Fig. 2 Time series (1957–1989) of the Sea of Okhotsk ice extent normalized anomaly (1) and normalized winter anomaly of SOI (2). (Positive values of SOI correspond to La Niña events, negative values correspond to El Niño events.)

NPI measuring intensity of Aleutian Low also has statistically significant positive unlagged cross-correlation with SOI for winter. In winter, NPI also has positive lagged cross-correlation with SOI taken for a previous summer (Table 3). Figure 1 shows that NPI varies in phase with air temperature at the Ust-Hairuzovo meteorological station. At the same time, NPI spectra calculated for monthly mean time series in summer have a decadal spectral maximum, which is also present in the winter time series of air temperature over the Sea of Okhotsk. The Okhotsk Sea ice extent shows a decadal maximum in the spectrum as well (Plotnikov, 1997).

It was earlier shown that the ENSO cycle is accompanied by South Asian Monsoon anomalies (Webster and Yang, 1992; Sekine, 1996) and by a change in the jet stream and the associated storm tracks which, in turn, alters the heat and vorticity fluxes caused by the transient eddies over the Northern Hemisphere (Branstator, 1995). Therefore, it is reasonable to suggest that ENSO and decadal scale variations in the Sea of Okhotsk are connected via both annual–biennial oscillations of

the Asian monsoon system and ocean–atmosphere interaction in the western mid-latitude Pacific.

Palmer et al. (1992) and Molteni et al. (1993) argued that, despite very large natural variability of the extratropical atmosphere circulation, there exist certain preferred regimes with rather persistent flow patterns presumably associated with the land–sea distribution and climatological planetary waves. The effect of tropical sea surface temperature forcing associated with the ENSO cycle alters the frequency of occurrence and stability of certain pre-existing regimes (*Learning to Predict Climate Variations Associated with El Niño and Southern Oscillation. Accomplishments and Legacies of the TOGA Program*, 1996).

Polyakova (1997) suggested six typical synoptic patterns of atmospheric circulation over the North Pacific based on heuristic analysis of daily sea surface pressure fields with a special consideration of positions of cyclone tracks and of the Aleutian Low and Subtropic High pressure centers. Choice of original pressure fields rather than averaged, for example, monthly data, gave patterns which keep

information on synoptic processes. They were earlier described in detail (Ponomarev et al., 1999), and similarity were emphasized over the North Pacific with known atmospheric circulation patterns such as the Pacific–North American (PNA), East–West (EW), and Zonal Dipole (ZD) patterns (Wallace and Gutzler, 1981; Barnston and Livezey, 1987). The calendar developed by Polyakova (1997) for the period from 1949 to 1998 reflects alternation of these patterns in time and is hereafter used as a base for composing monthly time series of their frequency of occurrence in days per month.

Considering low-frequency variations of oceanographic and meteorological characteristics in the Sea of Okhotsk, two most frequent meteorological situations are of particular interest (Polyakova, 1997; Ponomarev et al., 1999). They are the Okhotsk–Aleutian and Cyclones Over North Pacific situations (Figs. 3 and 4). The Okhotsk–Aleutian (OA) situation (Fig. 3) represents the classical meridional dipoles with a high pressure ridge over the central Pacific from the Subtropics to the Subarctic and low pressure over the eastern and western Pacific. Northward tracks of southern cyclones dominate over the western and eastern Pacific Ocean. As for the western Pacific, cyclones come from the Philippine Sea through the Kuroshio–Oyashio area to the Kuril adjacent to the Pacific, Japan and Okhotsk Seas.

Figure 5 shows OA normalized annual frequency of occurrence. The biennial variations are clearly seen on the plot, and they are also typical for all six types. The estimated polynomial trend also shows interdecadal oscillations with the period of about 30 years.

To reveal ENSO-scale variations, a cross-correlation was estimated between OA and CN frequency of occurrence and SOI time series. As oscillations are present for different time-scales, correlation coefficients should not be high. In fact, we had to try various sub-samples of the 1949–1998 time series to obtain the best correlation with SOI. Some examples are shown in Table 5. Nevertheless, positive unlagged correlation was found between OA occurrence and SOI in June and November. This means that the OA situation occurs more often when SOI reaches its highest positive values during the La Niña event in June or in November.

Cross-correlation of the OA situation occurrence was estimated with monthly mean air temperature at the meteorological stations around the Sea of Okhotsk. Both unlagged and lagged, with air temperature lagging one month behind OA, correlation coefficients were calculated. As shown in Table 6, all coefficients are positive, that is, the OA situation is warm for the Sea in fall, winter and spring. So, the OA situation, meridional for

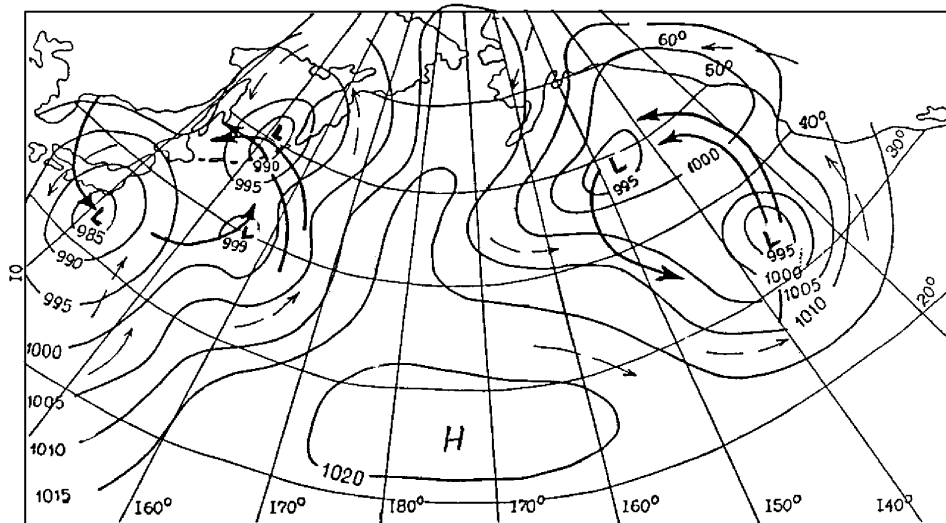


Fig. 3 Sea level pressure pattern corresponding to the Okhotsk–Aleutian synoptic situation. Air mass transport is shown by thin arrows, cyclone tracks are shown by thick arrows. (Reproduced from Polyakova (1997).)

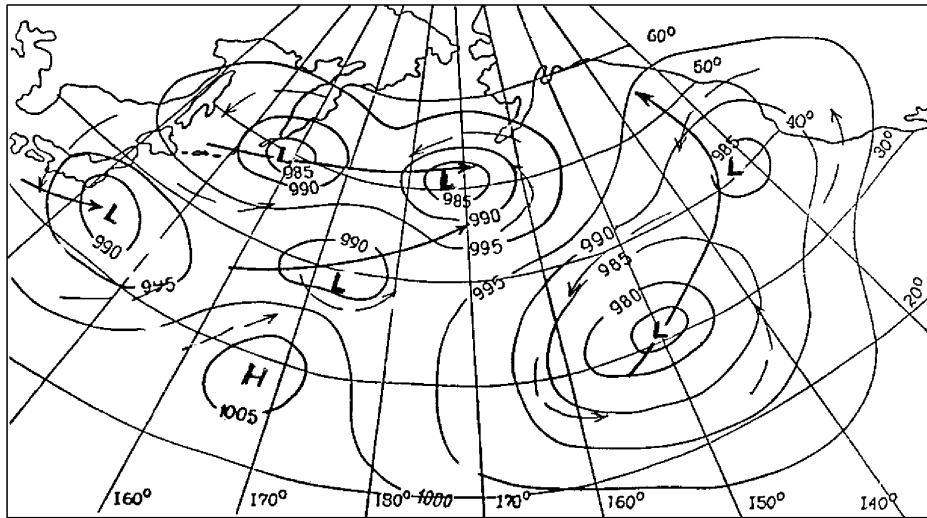


Fig. 4 Sea level pressure pattern corresponding to the Cyclones Over the North Pacific synoptic situation. Air mass transport is shown by thin arrows, cyclone tracks are shown by thick arrows. (Reproduced from Polyakova (1997).)

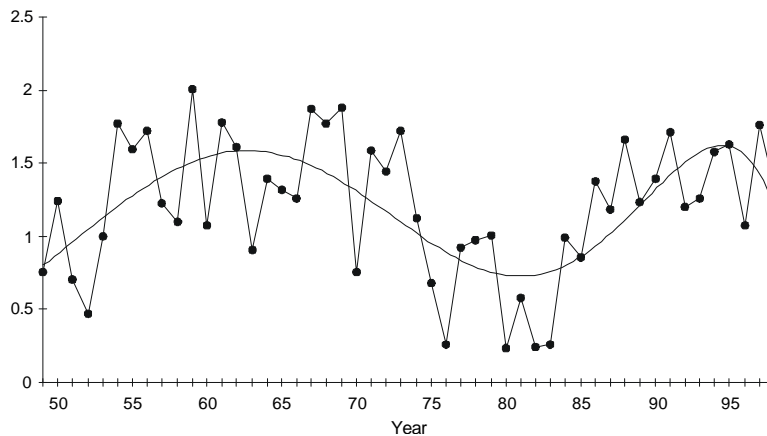


Fig. 5 Annual mean frequency of occurrence for the Okhotsk–Aleutian synoptic situation, normalized by root mean square difference. Polynomial trend of 6th order is also shown.

the whole North Pacific, corresponds to penetration of southern cyclones with characteristic weather patterns to the Northwest Pacific Margin and, in particular, over the Sea of Okhotsk. Positive correlation of OA occurrence with SOI means that decreased southern cyclones cool the Okhotsk Sea during El Niño events in fall or increased southern cyclones warm the Sea in fall after summer La Niña events.

The Cyclones Over the North Pacific (CN) synoptic situation (Fig. 4) is characterized by a meridional circulation pattern in the eastern Pacific with the western position of the Subtropic High Pressure, northward cyclone tracks over the Eastern Pacific, and eastward tracks over the Central and Western Pacific between latitudes of 40°–50°N. To the north of 50°N, cold air comes over the Okhotsk Sea from the Bering Sea and Siberia. The

CN occurrence has negative unlagged correlation with SOI for March, April, May, October and November (Table 5). Therefore, it occurs more often in spring and fall during El Niño events. The CN situation is cold for the Sea of Okhotsk in winter and spring as estimated cross-correlation with air temperature around the Sea shows (Table 7). So, increased occurrence of the CN situation in spring during El Niño events tends to cool the Sea.

A plot of CN normalized annual mean frequency of occurrence (Fig. 6) shows typical biennial variations as well as multiannual peaks. Averaging intervals between corresponding maximums which took place in 1950, 1958, 1970, 1985, and 1992 gives a period of 10 years, that is, decadal oscillations.

Table 5 Unlagged cross-correlation of the Okhotsk–Aleutian and Cyclone Over the North Pacific synoptic atmosphere situations occurrence (days per month) with SOI based on monthly mean time series. The 95%-confidence levels are also shown, calculated according to the Fisher test.

Data	SOI	Sample size	95% level
Okhotsk-Aleutian, June, 1962–1992	0.415	31	0.360
Okhotsk-Aleutian, June, 1956–1992	0.35	37	0.329
Okhotsk-Aleutian, November, 1949–1996	0.38	48	0.290
Okhotsk-Aleutian, November, 1949–1998	0.35	50	0.282
Okhotsk-Aleutian, November, 1952–1993	0.36	42	0.308
Cyclone over the North Pacific, March, 1959–1997	–0.55	39	0.320
Cyclone over the North Pacific, April, 1959–1997	–0.33	39	0.320
Cyclone over the North Pacific, May, 1949–1994	–0.33	46	0.294
Cyclone over the North Pacific, October, 1966–1994	–0.47	29	0.373
Cyclone over the North Pacific, November, 1949–1994	–0.31	46	0.294

Table 6 Cross-correlation between the Okhotsk–Aleutian synoptic atmosphere situation frequency of occurrence and air temperature at the meteorological stations around the Okhotsk Sea, calculated for monthly mean time series and summarized by seasons of the year. Both unlagged and lagged with air temperature 1 month lagging behind the synoptic situation correlation coefficients are shown. A 95%-confidence level for monthly mean time series for the period 1949–1990 is estimated as 0.308 based on the Fisher test.

Stations	Winter		Spring		Summer		Fall	
	Zero lag	1 month lag	Zero lag	1 month lag	Zero lag	1 month lag	Zero lag	1 month lag
Icha	0.35, 0.49	–	0.31, 0.34	0.47	–	–	0.37	–
Magadan	–	0.36	–	0.35	–	–	–	–
Ajan	–	0.41	–	–	–	–	0.32	–
Nikolaevsk	–	–	0.38	0.37	0.41	–	–	–
Alexandrovsk	–	0.31	0.40	0.36	–	–	–	–
Poronaysk	–	0.33	0.41, 0.49	0.51	–	–	0.33	–
Abashiri	0.35	0.38	0.31, 0.34	0.39	–	–	–	–
Nemuro	0.35	0.42	0.32, 0.37	0.44	–	–	–	–

Table 7 Cross-correlation of the Cyclone Over the North Pacific synoptic atmosphere situation frequency of occurrence with air temperature at meteorological stations around the Okhotsk Sea, calculated for monthly mean time series and summarized by seasons of a year. (A) columns show unlagged correlation coefficients, (B) columns show lagged correlation with air temperature 1 month lagging behind the synoptic situation. A 95%-confidence level for monthly mean time series form 1949 to 1990 is estimated as 0.308 based on the Fisher test.

Stations	Winter		Spring	
	A	B	A	B
Icha	–	–	–0.47	–0.33
Magadan	–	–	–	–0.31
Okhotsk	–	–	–0.33	–0.4
Ajan	–	–0.40	–0.35	–
Nikolaevsk	–	–	–0.32	–
Alexandrovsk	–	–0.32	–0.31	–
Poronaysk	–	–0.42	–0.38	–0.31
Abashiri	–0.31	–	–	–
Nemuro	–0.33	–	–	–

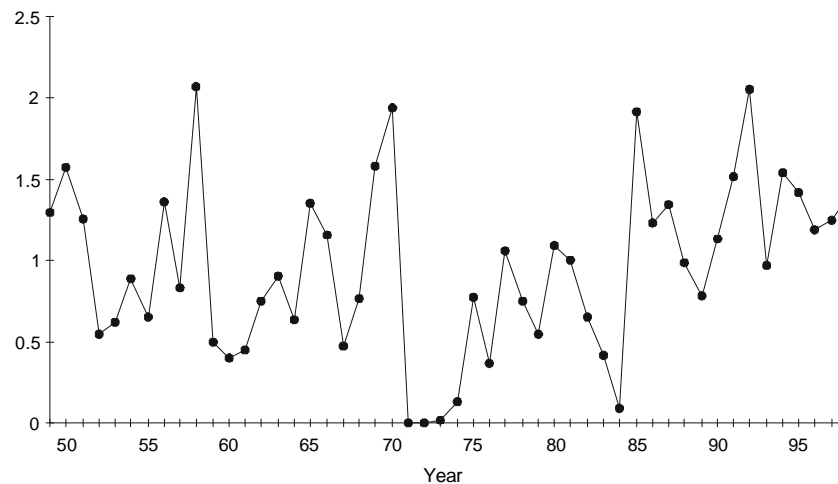


Fig. 6 Normalized annual mean frequency of occurrence for the Cyclones Over the North Pacific.

It is worth noting that the occurrence of the rare Southern-Zonal (SZ) situation seems to be related to the ENSO cycle. The SZ situation (Fig. 7) corresponds to a zonal dipole with high pressure over the Bering Sea and Alaska, extreme southern position of the subarctic low pressure system, eastward cyclone tracks in the subtropic Pacific area, and northeastward cyclone tracks over the subarctic eastern Pacific. The SZ situation may not occur at all during periods from few months to 2–3 years but, when it does occur, its duration (10–20 days) is comparable with the duration of frequent situations like the OA and CN ones (Fig. 8). The SZ situation shows increased occurrence between

typical ENSO cycles and huge occurrence in the 1–2 years before strong El-Niño events, particularly before winters of 1957–1958, 1972–1973, 1982–1983 and 1997–1998 (Fig. 8). As a whole, the highest SZ occurrence was observed in 1953, 1957, 1962–1963, 1968, 1971, 1972, 1974, 1977, 1979, 1981, 1985, 1989, 1993, and 1996–1997, which gives a mean period of 3.2 years consistent with the ENSO cycle. The SZ situation lasted 24 days in August 1996, its maximum occurrence during 1949–1998 (Fig. 8).

Thus, El Niño (La Niña)-accompanying processes in the Northwest Pacific result in cooling (warm-

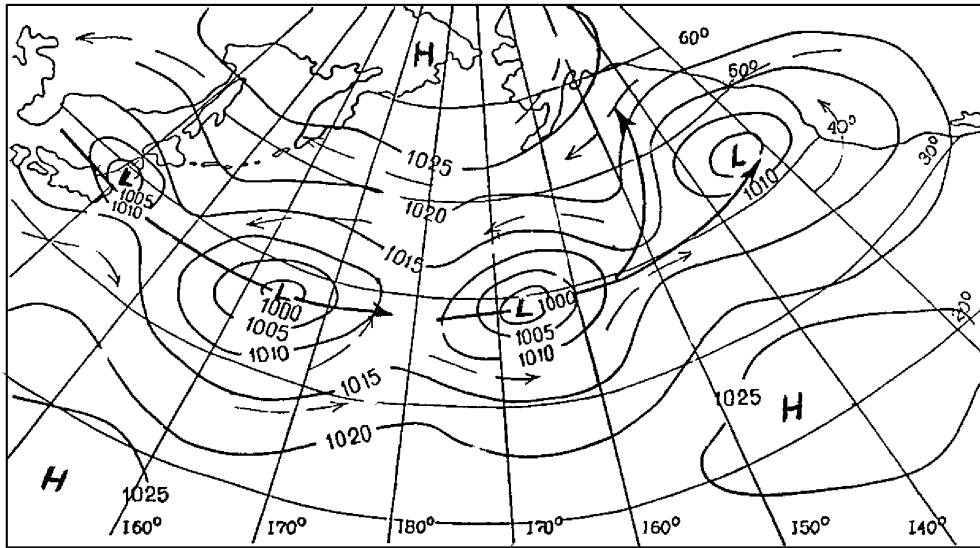


Fig. 7 Sea level pressure pattern corresponding to the Southern-Zonal synoptic situation. Air mass transport is shown by thin arrows, cyclone tracks are shown by thick arrows

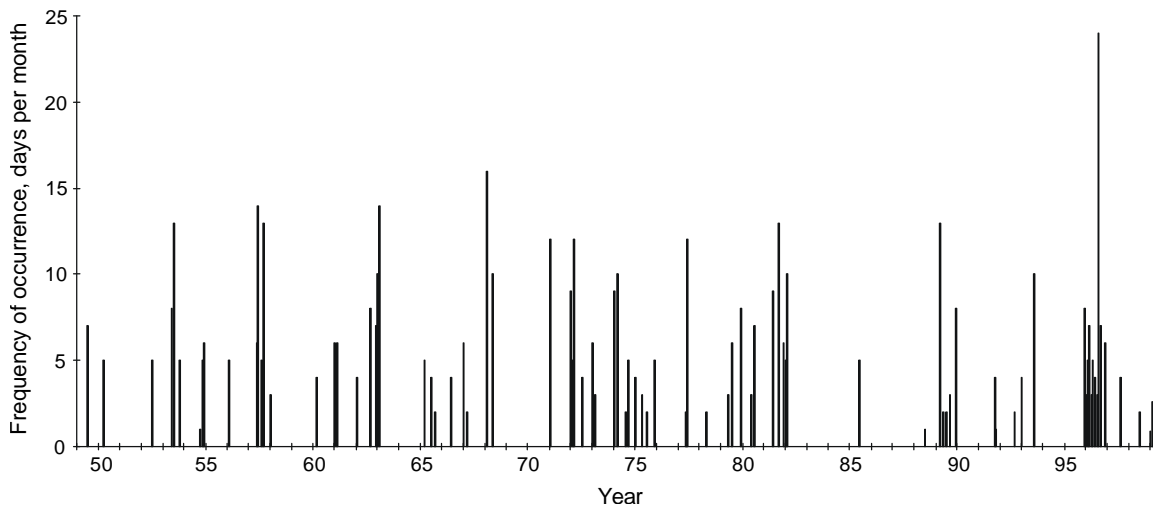


Fig. 8 Time series of monthly occurrence of Southern-Zonal synoptic situation for the period of 1949–1998 in days per month.

ing) the Sea of Okhotsk through changing occurrence of certain atmosphere circulation patterns. At the same time, correlation between air temperature around the Sea of Okhotsk and SOI with a lag of about half a year may be associated with the Northwest Pacific Ocean memory in a seasonal cycle.

References

- Barnston, A.G. and Livezey, R.E. 1987. Classification, seasonality and persistence of low-frequency atmospheric circulation patterns. *Mon. Weather Rev.*, 115, 1083–1125.
- Branstator, G.W. 1995. Organization of stormtrack

- anomalies by recurring low frequency circulation anomalies. *J. Atmos. Sci.*, 52, 207–226.
- Learning to Predict Climate Variations Associated with El Niño and Southern Oscillation. Accomplishments and Legacies of the TOGA Program.* 1996. National Academy Press, Washington, 235 pp.
- Molteni, F., Ferranti, L. Palmer, T.N. and Viterbo, P. 1993. A dynamical interpretation of the global response to equatorial Pacific sea surface temperature anomalies. *J. Climate*, 6, 777–795.
- Nakamura, H., Lin, G. and Yamagata, T. 1997. Decadal climate variability in the North Pacific during the recent decades. *Bull. Amer. Meteorol. Soc.*, 78(10), 2215–2225.
- Palmer, T.N., Brankovic, C., Viterbo, P. and Miller, M.J. 1992. Modeling interannual variations of summer monsoons. *J. Climate*, 5, 399–417.
- Plotnikov, V.V. 1997. Space–time relations between ice conditions in the Far Eastern Seas. *Meteorol. Gidrol.*, 3, 77–85. (in Russian)
- Polyakova, A.M. 1997. Types of atmospheric circulation over the North Pacific and climate variations in the North Pacific. pp. 98–105. In *Pacific Oceanol. Inst. Proc. of Annual Session, 1994.* Dalnauka, Vladivostok, Russia. (in Russian)
- Ponomarev, V.I., Trusenkova, O.O., Trousenkov, S.T., Kaplunenko, D.D., Ustinova, E.I. and Polyakova, A.M. 1999. The ENSO Signal in the Northwest Pacific. pp. 9–32. In *Proc. of the 1998 Science Board Symposium on the Impacts of the 1997/98 El Niño Event on the North Pacific Ocean and its Marginal Seas, PICES Sci. Rep. No. 10,* Sidney, B.C., Canada.
- Sekine, Y. 1996. Anomalous Oyashio intrusion and its teleconnection with Subarctic North Pacific circulation, sea ice of the Okhotsk Sea and air temperature of the northern Asian continent. pp. 177–187. In *Proc. of the Workshop on the Okhotsk Sea and Adjacent Areas, PICES Rep. No. 6,* Sidney, B.C. Canada.
- Sekine, Y. and F. Yamada, Y. 1996. Atmosphere and ocean global teleconnection around the Okhotsk Sea. pp. 148–150. In *The Eleventh Intl. Symp. on Okhotsk Sea and Sea Ice, Abstracts,* 25–28 February 1996, Mombetsu, Hokkaido, Japan.
- Wallace, J.M. and Gutzler, D.S. 1981. Teleconnections in the geopotential height field during the Northern Hemisphere winter. *Mon. Weather Rev.*, 109, 784–812.
- Webster, P.J. and Yang, S. 1992. Monsoon and ENSO: Selectively interactive systems. *Quart. J. Roy. Meteorol. Soc.*, 118, 877–926.